Nanowire deformation

DOI: 10.1002/smll.200700052

## Shear Stress Measurements on InAs Nanowires by AFM Manipulation**

*Michael Bordag,* Aline Ribayrol, Gabriela Conache, Linus E. Fröberg, Struan Gray, Lars Samuelson, Lars Montelius, and Hakan Pettersson*

Nanowires (NWs) have in recent years attracted considerable attention due to their interesting fundamental properties and the exciting prospects for using these materials in future electronic and photonic applications.[1] For example, nanoscale field-effect transistors,[2–4] inverters[5–6] and more complex logic gates[4] have been demonstrated using well-defined NW building blocks. Furthermore, it has recently been shown that it is possible to form heterostructures in NWs[5] facilitating one-dimensional (1D) electronics, for example, resonant tunneling diodes[7] and single-electron transistors.[8] For photonic applications, LEDs,[3] lasers,[9] and infrared photodetectors[10–11] have also been assembled using NWs.

Devices based on NWs can be of two types: vertical or lateral. Although vertical device designs may be the obvious choice for NWs, which grow vertically from the surface, interesting lateral devices such as crosslinked electronics can be made by depositing the NWs horizontally on a substrate using a dry technique or from a dispersion. Placing NWs at predetermined positions in a controlled manner requires an understanding of the adhesion and friction forces between the NWs and the surface. In addition to this, the microscopic origin of friction is interesting from a fundamental point of view. It is for instance known that at the sub-micrometer scale the friction force, $F_{\mathrm{lateral}}$, is proportional to the contact area $A$ rather than to the load force, that is, $F_{\mathrm{lateral}} = \sigma A$.[12–14]

In this paper, we present a novel method for investigating the shear stress $\sigma$ between InAs NWs and a $SiO_2$ surface. The proposed “method of the most-bent state” rests on the observation that for an ideal elastically deformed wire pinned by adhesion forces to a flat surface and in equilibrium between static friction forces and restoring elastic forces, the most tightly bent regions contain information about the maximal static friction force, that is, about the shear stress. Experimentally, the NWs are bent in a controlled manner using the tip of an AFM. After the manipulation, the most-bent state can be determined by visual inspection of AFM micrographs. Assuming bulk values for the Young’s modulus, the shear stress can be obtained from a straightforward analysis according to the standard theory of elasticity. We apply the method in this paper only to InAs nanowires, however the method is quite general and it can be expected to work for other wires as well.

To fabricate the NWs, size-selected gold particles were produced with an aerosol method,[15] and deposited on an InAs(111)B substrate. The substrate was subsequently transferred into a chemical beam epitaxy growth chamber. Prior to growth, the substrate oxide was removed by heating the substrate under As pressure. The growth sources used were trimethylindium (TMIn) and precracked tertiarybutylarsine (TBAs), which enter the growth chamber as molecular beams.[5] The resulting nanowires are about 50 nm in diameter and 3 μm in length. After growth, the wires were removed from the substrate and transferred to a silicon substrate with a 330-nm-thick $SiO_2$ layer. The transfer was carried out by mechanically wiping off the wires from the substrate using a cleanroom wipe, followed by brushing off the NWs from the wipe onto the $SiO_2$ layer. The manipulation and imaging of the NWs were performed using a Dimension 3100 Nanoscope IIIA microscope from Veeco, equipped with rectangular-shaped cantilevers with a nominal spring constant of about 40 $\mathrm{N\,m^{-1}}$.

To bend the NWs in a gentle controlled manner, the following AFM manipulation scheme was employed. After imaging of the surface with randomly distributed NWs, a single NW was selected and a manipulation force was applied at a predetermined position along the wire. In the trace scan, tapping-mode imaging was carried out at a predetermined distance above the surface (positive set-point). In the retrace scan, the $z$-setpoint was decreased (corresponding to a smaller tip–surface distance) and the oscillator driving voltage set to zero. This procedure was repeated along the same scan line, continuously decreasing the retrace $z$-setpoint in small steps, until a movement of the NW was observed in the AFM line scan data. The distance swept by the tip was sufficient to enable the NW to be bent beyond the point of the “most-bent state”, after which it relaxes to the equilibrium configuration where the friction forces balance the elastic restoring forces.

The shear stress $\sigma$ (i.e., the lateral static friction force, $F_{\mathrm{lateral}}$, per unit area) is considered to be a more fundamental quantity than the friction coefficient at a macroscopic level. While friction at the macroscopic level depends on a variety of factors, for example, the surface roughness, more fundamental physical principles are addressed on a microscopic level when we are concerned with friction between atomically flat surfaces. Microscopic friction may depend on a number of factors including residual surface contamina-

[*] Dr. M. Bordag
Institute for Theoretical Physics, Leipzig University
Postbox 100 920, 04009 Leipzig (Germany)
Fax: (+49) 341-973-2548
E-mail: Michael.Bordag@itp.uni-leipzig.de

Dr. M. Bordag, G. Conache, Prof. H. Pettersson
Center for Applied Mathematics and Physics
Halmstad University, Box 823, SE-301 18 Halmstad (Sweden)

Dr. A. Ribayrol, G. Conache, L. E. Fröberg, Dr. S. Gray,
Prof. L. Samuelson, Prof. L. Montelius, Prof. H. Pettersson
Solid State Physics/The Nanometer Structure Consortium
Lund University, Box 118, 22100 Lund (Sweden)

[**] The authors acknowledge financial support from EC (6th FP NMP4-CT-2005-017071), the Swedish Research Council under Grant No. 621-2004-4439, the Swedish National Board for Industrial and Technological Development, the Office of Naval Research, and the Swedish Foundation for Strategic Research.


© 2007 Wiley-VCH Verlag GmbH & Co. KGaA, Weinheim

tion and chemical bonds between the bodies. Also rolling motion caused by locking of the crystal structure can play a role, as recently found in ab initio calculations,[16] as well as in experiments.[17] For a better understanding it is necessary to measure the dependence of the shear stress on various parameters, for example, surface properties, contact area, and temperature. There are a number of lateral-force measurement techniques reported in the literature. Most of them measure the torsional deflection of an AFM tip moving in contact with the surface.[18–19] Others move nanoparticles (such as $MoO_3$ crystals) attached to the tip over a surface, thus avoiding uncertainties in the shape of the tip.[20] In general, the shear stress has been found to be proportional to the contact area, while in some cases it was found to be proportional to the load force.

An interesting novel alternative to conventional lateral force measurements is to use the elastic restoring force of a bent NW for probing the shear stress. A prerequisite for this approach is that the wires behave as ideal elastic objects, and that elastic properties such as the Young's modulus are known. Several reports can be found in the literature discussing these parameters (see for example Ref. [21] and references therein). From these studies it is evident that, in general, the bulk value of the Young's modulus can not be assumed to be valid for nanowires. Instead it has been experimentally shown that the Young's modulus for NWs with a diameter below 200 nm can be smaller or larger than the bulk value depending on the material of the wire. Also, theoretical predictions are far from being conclusive.[22–23] In the present work, the diameter of the InAs NWs is about 50 nm. Since no experimental data is available for the Young's modulus of such thin wires, we assume the bulk value of $Y = 58$ GPa.

In order to describe the new method suggested in the present work in more detail, we consider an ideal elastic NW pinned by adhesion forces to a perfectly flat surface. The adhesion forces and the lateral friction forces are assumed to be evenly distributed along the length of the wire. Pinned to the surface, the wire may be in different bent states characterized by the radius of curvature, $R(z)$, $z$ being a location along the wire. The bending of the wire causes a corresponding elastic restoring force $F(z)$. We consider the situation when this restoring force is in equilibrium with the static friction force, that is, all dynamic effects are excluded. By measuring the radius of curvature at different positions along the wire, the friction force ranging from zero to some maximum can be probed locally. Evidently, the maximum friction force (shear stress) is present at a position where the wire is most strongly bent – that is, where it exhibits the smallest radius of curvature. A bent state with an even smaller radius of curvature would experience an elastic force larger than the friction force and so after the manipulation force from the AFM tip is removed the NW would slide until the restoring force balances the elastic force and equilibrium is reached. The most-bent state can be a local state or a global state over the whole length of the wire. In the latter case the shape of the wire would be circular.

A necessary prerequisite for our approach is that the NW is still in the elastic region of deformation, even in the most-bent state. Whether this is the case depends on the relation between the friction forces and the restoring elastic force. On one hand, if the friction is too strong bending may appear beyond the elastic region, even up to fracture. In the examples considered here, the radius of curvature is more than 10-times the radius of the wires, so an assumption of elastically deformed wires is likely to be valid. On the other hand, if the friction is too weak no bending can be observed. In this case the analyses would only give an upper bound for the friction force, which obviously depends on factors such as the precision of the curvature measurement. Of course, the question whether we are in the elastic region or not cannot be finally answered here. There are most likely defects in the NWs. However, even repetitive bending of the wires did not result in any observable kinks in the curved shape, from which we conclude that the defects do not introduce any substantial plastic floating.

The determination of the friction force from the most-bent state is in fact quite straightforward. A bent wire stores an elastic energy $U$ given by the known formula

$$U = \frac{YI}{2} \int \frac{1}{R(z)^2} dz \tag{1}$$

where $Y$ is the Young's modulus and $I$ is the geometric moment of inertia. The NWs under consideration are known to have a hexagonal cross section[24] for which $I = \frac{5\sqrt{3}}{144} D^4$ with respect to either of the two possible symmetry axes of the hexagonal section. Here, the diameter $D$ is defined as the distance between two parallel edges of the hexagon. $R(z)$ is the local radius of curvature. The integration is over the length of the wire. Assuming the NW to be in a "global most-bent state", it forms a circle and the formula given above transforms into

$$U = \pi \frac{YI}{R} \tag{2}$$

Differentiating this expression with respect to the radius and reversing the sign yields the force acting on the whole circumference. Dividing this force by the circumference of the wire gives the force per unit length,

$$F = \frac{YI}{2R^3} = \frac{5\sqrt{3}\, YD^4}{288\, R^3} \tag{3}$$

The force given in Equation 3 is thus the friction force acting in the most-bent state. This can also be obtained by taking the variational derivative with respect to $R(z)$ from the elastic energy $U$ (Equation 1). For later convenience, Equation 3 is rewritten in more appropriate dimensions. The force per unit length, measured in units of $\mathrm{nN\,nm^{-1}}$, is given by

$$\frac{F}{(\mathrm{nN/nm})} = \frac{5\sqrt{3}}{288} \frac{Y}{\mathrm{GPa}} \frac{(D/\mathrm{nm})^4}{(R/\mathrm{nm})^3} \tag{4}$$

A number of AFM micrographs of bent NWs have been analyzed using Equation 4. Figure 1 shows a typical micrograph of a NW before and after applying the manipulation


© 2007 Wiley-VCH Verlag GmbH & Co. KGaA, Weinheim

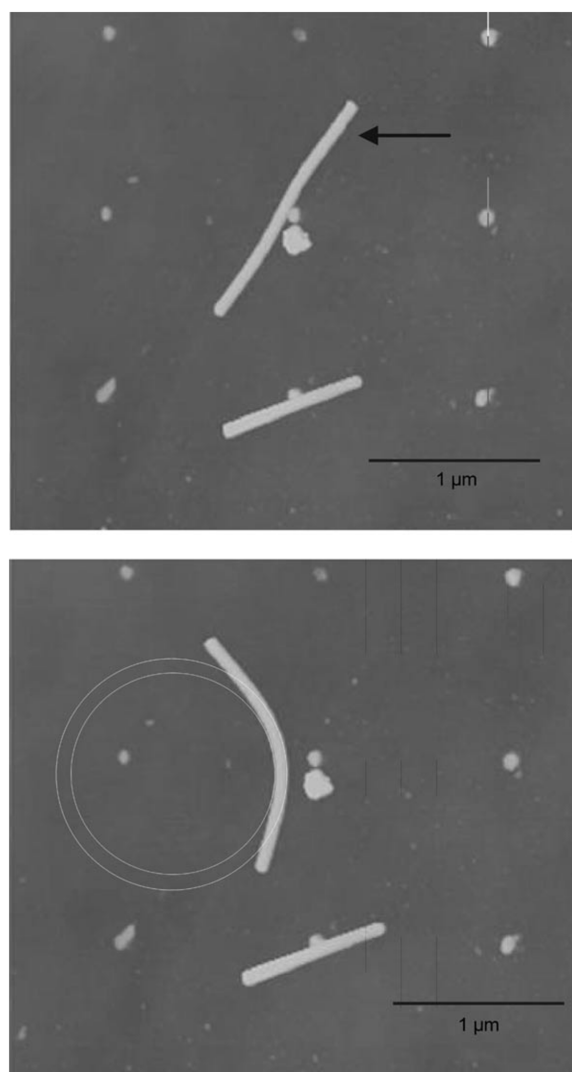


**Figure 1.** Top: AFM micrograph of NWs on a $SiO_2$ surface before manipulation. The black arrow indicates the force vector to be applied to the selected NW. Bottom: The NW after manipulation. The circles are drawn to determine the inner and outer curvature radii.

force. The arrow in the left panel shows the line along which the AFM tip moved during the manipulation step. The distance moved by the tip was substantial, implying that the wire must have been bent even further than shown in the image in the right panel. This implies that the wire was indeed bent beyond the most-bent state, after which it relaxed to equilibrium. It should be noted that the relaxation is overdamped since inertia is negligible at these length scales. Further we notice that the "free arms" of the bent wires are quite short, so there cannot be any disregarded forces that are amplified via a long lever arm. To deduce the radius of curvature of the most-bent state, an inner and an outer circle were positioned using a standard drawing software tool on the micrograph at the location of the most curved part of the NW. The precision of this procedure is estimated to be about 10%. The mean value of the radii of the two circles gives the radius of curvature $R$. The diameters of the wires were taken from height profiles obtained by AFM. Table 1 displays the results of extracting the friction forces for different NWs.

From Table 1 it is evident that all wires have a diameter $D$ close to 50 nm, and a radius of curvature of about 700 nm. A significantly smaller radius of curvature was not observed in this study. From this it is concluded that most-bent states have indeed been identified. Also, as already mentioned above, the radii of curvature are all more than 10-times larger than the diameter of the wires, so that they are expected to be in the elastic regime. The forces given in Table 1 were calculated using Equation 4. We conclude that the typical friction force (and thus force needed to move or to bend wires) is on the order of a few tens of piconewtons per nanometer. For a 1 µm NW this translates into a few tens of nanonewtons.

The shear stress $\sigma$ can be obtained from this force by dividing by the transversal contact length of the NW, which is $D/\sqrt{3}$. Here it is assumed that the wire rests with a flat side on the surface. This assumption is plausible since the elastic restoring force does not depend on the orientation of the wire as discussed above, and the adhesion force is thus expected to bind the flat side of the wire to the $SiO_2$ surface. Further support for this assumption is observed in Figure 2 showing a close-up AFM image of a wire after it has been bent. Interestingly, two faint traces can be observed on the $SiO_2$ surface corresponding to the position where the wire was located prior to manipulation. The separation between the traces is comparable to the width of the flat side of the wire, and we attribute the traces to a shallow oxide present at the borders of the wire before it was bent.

The corresponding values of the shear stress $\sigma$ are entered in the last column of Table 1. The mean value of the shear stress is $\bar{\sigma}=0.99$ MPa, and the corresponding dispersion is $\Delta\sigma=\sqrt{\frac{1}{N}(\sigma_i-\overline{\sigma}_i)^2}=0.25$ MPa. The values found for the shear stress are two orders of magnitude smaller than values obtained in many measurements of the friction force between an AFM tip and a substrate, as well as the friction forces involved in moving larger-sized nanoparticles on a substrate (see other literature for details[19,25–27]). On the other hand, in several reported measurements with smaller-sized particles values of a few MPa were indeed found[20,28].

**Table 1.** Friction forces and corresponding shear stresses obtained for different NWs.

| NW No. | Radius of curvature $R$ [nm] | NW diameter $D$ [nm] | Friction force $F$ [pN nm$^{-1}$] | Shear stress $\sigma$ [MPa] |
|---|---|---|---|---|
| 1 | 798 | 46 | 16 | 0.59 |
| 2 | 665 | 48 | 30 | 1.10 |
| 3 | 694 | 48 | 27 | 0.97 |
| 4 | 622 | 48 | 39 | 1.41 |
| 5 | 690 | 49 | 30 | 1.06 |
| 6 | 693 | 50 | 33 | 1.13 |
| 7 | 794 | 51 | 23 | 0.80 |
| 8 | 786 | 52 | 27 | 0.90 |


© 2007 Wiley-VCH Verlag GmbH & Co. KGaA, Weinheim

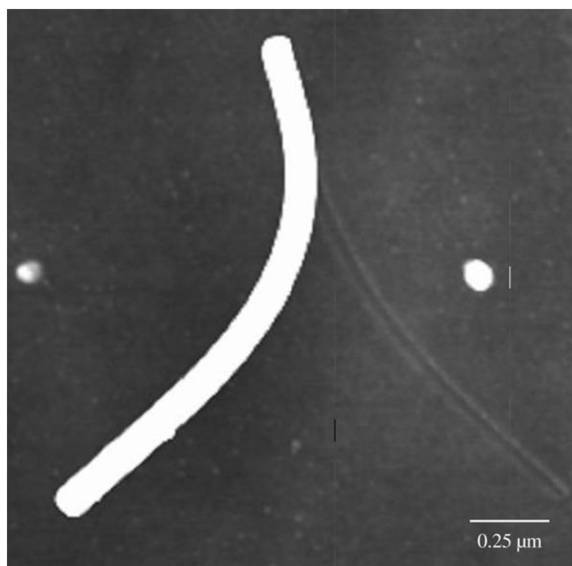


**Figure 2.** AFM micrograph of a NW after manipulation. The two faint traces in the oxide provide support for the assumption that the hexagonal NWs rest with the flat side on the $SiO_2$ surface.

In addition, in most experiments a load force was applied, which tends to increase the contact area and the shear stress. In our case, however, no load force is present during the relaxation of the wire and the normal force is solely due to adhesion. Another important aspect to consider is the existence of a thin water film on the $SiO_2$ surface. These experiments have been carried out in air and thus the water film could modify the friction forces between the NW and the surface.

In conclusion, a novel approach to measure the lateral friction force between elastic InAs nanowires and a $SiO_2$ surface is reported. The method is based on the fact that an elastically deformed wire is kept in equilibrium by counterbalancing static friction forces and restoring elastic forces. From the radius of curvature of the NW the friction force can be deduced, assuming that the elastic properties of the wire are known. The method offers a new path to determine important interactions between nanoscale objects and surfaces of different materials.

**Keywords:**
atomic force microscopy · deformation · indium arsenide · nanowires

[1] J. T. Hu, T. W. Odom, C. M. Lieber, *Acc. Chem. Res.* **1999**, *32*, 435.
[2] Y. Cui, C. M. Lieber, *Science* **2001**, *291*, 851.
[3] X. F. Duan, Y. Huang, Y. Cui, J. F. Wang, C. M. Lieber, *Nature* **2001**, *409*, 66.
[4] Y. Huang, X. F. Duan, Q. Q. Wei, C. M. Lieber, *Science* **2001**, *291*, 630.
[5] M. T. Bjork, B. J. Ohlsson, T. Sass, A. I. Persson, C. Thelander, M. H. Magnusson, K. Deppert, L. R. Wallenberg, L. Samuelson, *Appl. Phys. Lett.* **2002**, *80*, 1058.
[6] Y. Huang, X. F. Duan, Y. Cui, L. J. Lauhon, K. H. Kim, C. M. Lieber, *Science* **2001**, *294*, 1313.
[7] M. T. Bjork, B. J. Ohlsson, C. Thelander, A. I. Persson, K. Deppert, L. R. Wallenberg, L. Samuelson, *Appl. Phys. Lett.* **2002**, *81*, 4458.
[8] C. Thelander, T. Martensson, M. T. Bjork, B. J. Ohlsson, M. W. Larsson, L. R. Wallenberg, L. Samuelson, *Appl. Phys. Lett.* **2003**, *83*, 2052.
[9] M. H. Huang, S. Mao, H. Feick, H. Q. Yan, Y. Y. Wu, H. Kind, E. Weber, R. Russo, P. D. Yang, *Science* **2001**, *292*, 1897.
[10] H. Pettersson, J. Tragardh, A. I. Persson, L. Landin, D. Hessman, L. Samuelson, *Nano Lett.* **2006**, *6*, 229.
[11] O. M. Braun, A. G. Naumovets, *Surf. Sci. Rep.* **2006**, *60*, 79.
[12] M. R. Falvo, R. Superfine, *J. Nanopart. Res.* **2000**, *2*, 237.
[13] J. F. Wang, M. S. Gudiksen, X. F. Duan, Y. Cui, C. M. Lieber, *Science* **2001**, *293*, 1455.
[14] D. S. Grierson, E. E. Flater, R. W. Carpick, *J. Adhes. Sci. Technol.* **2005**, *19*, 291.
[15] M. H. Magnusson, K. Deppert, J. O. Malm, J. O. Bovin, L. Samuelson, *J. Nanopart. Res.* **1999**, *1*, 243.
[16] J. D. Schall, D. W. Brenner, *Mol. Simul.* **2000**, *25*, 73.
[17] M. R. Falvo, J. Steele, R. M. Taylor, R. Superfine, *Phys. Rev. B* **2000**, *62*, R10665.
[18] R. W. Carpick, N. Agrait, D. F. Ogletree, M. Salmeron, *J. Vac. Sci. Technol. B* **1996**, *14*, 1289.
[19] O. Pietrement, M. Troyon, *Surf. Sci.* **2001**, *490*, L592.
[20] P. E. Sheehan, C. M. Lieber, *Science* **1996**, *272*, 1158.
[21] C. Q. Chen, Y. Shi, Y. S. Zhang, J. Zhu, Y. J. Yan, *Phys. Rev. Lett.* **2006**, *96*, 075505.
[22] D. E. Segall, S. Ismail-Beigi, T. A. Arias, *Phys. Rev. B* **2002**, *65*.
[23] E. W. Wong, P. E. Sheehan, C. M. Lieber, *Science* **1997**, *277*, 1971.
[24] N. Skold, J. B. Wagner, G. Karlsson, T. Hernan, W. Seifert, M-E. Pistol, L. Samuelson, *Nano Lett.* **2006**, *6*, 2743.
[25] M. Enachescu, R. J. A. van den Oetelaar, R. W. Carpick, D. F. Ogletree, C. F. J. Flipse, M. Salmeron, *Tribol. Lett.* **1999**, *7*, 73.
[26] M. A. Lantz, S. J. Oshea, M. E. Welland, K. L. Johnson, *Phys. Rev. B* **1997**, *55*, 10776.
[27] C. Ritter, M. Heyde, B. Stegemann, K. Rademann, U. D. Schwarz, *Phys. Rev. B* **2005**, *71*.
[28] E. Meyer, R. Luthi, L. Howald, M. Bammerlin, M. Guggisberg, H. J. Guntherodt, *J. Vac. Sci. Technol. B* **1996**, *14*, 1285.

Received: January 22, 2007
Published online on July 19, 2007


© 2007 Wiley-VCH Verlag GmbH & Co. KGaA, Weinheim